RAPID COMMUNICATIONS

PHYSICAL REVIEW E VOLUME 52, NUMBER 6 DECEMBER 1995

Molecular dynamics–continuum hybrid computations: A tool for studying complex fluid flows

Sean T. O'Connell and Peter A. Thompson*

Department of Mechanical Engineering and Materials Science, and Center for Nonlinear Dynamics and Complex Systems, Duke University, Durham, North Carolina 27708-0300

(Received 1 March 1995)

A generic algorithm is presented for coupling a molecular dynamics (MD) simulation to a continuum-based computation for a fluid system. The coupling is achieved by constraining the dynamics of fluid molecules in the vicinity of the MD-continuum interface. The validity of the hybrid method is demonstrated for a unidirectional, startup flow of a simple fluid near a solid surface. By vastly extending the length scales accessible in MD simulations, the method makes possible an efficient study of the macroscopic ramifications of microscopic interfacial phenomena.

PACS number(s): 02.70.−c, 47.11.+j, 68.45.−v, 83.20.Jp

With the advent of high speed computing, nonequilibrium molecular dynamics (MD) simulations have proven to be a valuable tool in the study of fluids. In addition to probing the constitutive behavior of polymeric and colloidal liquids, they have also been used to model a variety of complex, microscopic hydrodynamic phenomena [1]. Recent applications include studies of convection, coalescence, spreading and wetting, and instabilities in boundary lubrication. One of the great strengths of MD is that it does not require phenomenological input such as boundary conditions (BCs) and constitutive laws. It is also capable of modeling flow in regions where there are large gradients in velocity and density [1]. Furthermore, MD simulations provide detailed structural information about the fluid, which can be used to understand the dynamics of the flow.

Although extremely useful, MD simulations are computationally intensive and therefore can only probe phenomena over relatively short time and length scales. For example, simulations of hydrodynamic phenomena in a simple liquid on a length scale of order 15 nm are typically limited to time scales of order 10 ns when performed on a modern workstation. Such limitations often make it difficult to compare MD results with experimental observations. They also make MD simulations impractical as a tool in engineering design.

In this paper, we describe a computational technique that extends the length scales accessible in MD simulations of fluids. The technique involves coupling an MD simulation in one region to a continuum-based computation in another. The MD portion of the hybrid computation is utilized in regions where structural inhomogeneities and other complex features prevent a simple continuum description of the fluid. Typically, such regions are localized near interfaces (within 50 Å) [1,2]. Outside of this domain, in the smoothly varying region, a Navier-Stokes description is used. In linking these two regions, the MD simulation can effectively access arbitrarily large length scales typical of macroscopic flows without additional computational effort.

Discrete-continuum computations in and of themselves are not a new tool in the study of fluids. A common implementation entails embedding a discrete computation within a continuum model to sample and supply information about variations in thermodynamic properties. These have been particularly useful in modeling chemically reactive flows [3]. In contrast, our hybrid computation involves the explicit dynamical coevolution of two spatially distinct domains. A similar type of computation has been developed to study shocks in rarified gas flows. It consists of coupling a direct simulation Monte Carlo algorithm to a continuum model [4]. As in the algorithm presented here, the discrete model is utilized in regions where continuum assumptions break down.

The most important concern in any discrete-continuum hybrid computation is the continuity of thermodynamic and transport properties across the interface between the two descriptions. This interface is illustrated in Fig. 1 and is referred to in this work as the hybrid solution interface or HSI. In the case of an MD-continuum hybrid computation, the termination of the spatial extent of the MD induces local structure in the fluid, particularly at liquid densities [1,2]. Since this structure precludes continuity, we extended the MD portion of the computation beyond the HSI, introducing an overlap region. The fluid particles within this region are represented by the open circles in Fig. 1. Provided this overlap is large enough to screen the HSI from the effects of the termination, the density (and temperature) will be continuous.

For an isothermal fluid, the relevant transport quantities are mass and momentum flux. Continuity of mass flux at the

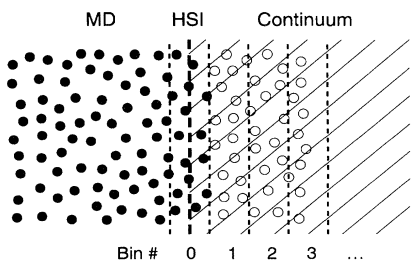

FIG. 1. Schematic for the region near the MD-continuum interface. Bins used for averaging particle velocities in the overlap region are delineated by the dashed lines.

*Also at Department of Physics, Duke University.

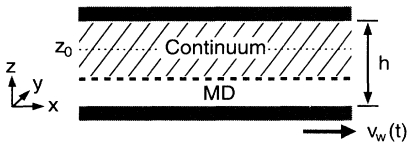

FIG. 2. Schematic of the flow geometry used to test the hybrid algorithm. The dashed line represents the region near the HSI, and h denotes the distance separating the two planar walls. The dotted line at z_0 indicates the spatial extent of the MD computation.

HSI is achieved by supplying the continuum with spatially and temporally averaged particle velocities. In the context of Fig. 1, this averaging is carried out over the zeroth bin, and the resultant average becomes the velocity BC for the continuum.

In contrast to mass flux, ensuring the continuity of momentum flux at the HSI is a more subtle issue. The difficulty arises when trying to reconcile the stress supplied by the continuum within the MD description [1]. Unlike in a continuum model, a local constitutive representation is not assumed in the MD. Instead, the state of stress is an explicit computation of the momentum flux of molecules across a surface element moving with the local velocity and the forces acting between molecules on either side of the surface element [5]. These two contributions make up the kinetic and virial terms of the microscopic stress tensor, respectively [6]. In order to impose a continuity of stress at the HSI, we would therefore need to know *a priori* over what length and with what magnitude to apply the necessary corrective forces. Although feasible, this would introduce a high degree of subjectiveness into the calculations.

In our hybrid scheme, the continuity of stress is achieved by exploiting the presence of the overlap region. In order that the state of stress at a point in the MD description be the same as that of the local continuum, the thermodynamic properties and the velocity field must be consistent with the continuum within a radius of a few molecular diameters. As described above, the overlap region was introduced to ensure the consistency of the thermodynamic properties in the vicinity of the HSI. To guarantee that the velocity field is also consistent, the average momentum of the overlap particles is relaxed to that of the corresponding continuum fluid element through the application of constraint dynamics. This constraint allows the momentum transport across the HSI to be handled by the interactions of the MD particles *themselves* not by an empirical or *ad hoc* corrective field. Thus, the overlap particles (though not actually a part of the hybrid solution) facilitate the recovery of a continuous state of stress across the HSI.

To demonstrate the validity of our hybrid scheme, we used it to model the startup flow of an isothermal Newtonian fluid in a planar Couette cell. This flow provides an excellent test for the scheme because the stress and velocity fields are nonlinear in both space and time. Furthermore, the hybrid solution can be easily compared to full MD and continuum computations. The geometry of the system is shown in Fig. 2. The walls of the cell were oriented parallel to the xy plane and separated by distance h. Periodic BCs were imposed in the x and y directions. The fluid was sheared by translating the lower wall in the $\hat{x}$ direction with velocity $v_w(t)$. The MD portion of the hybrid computation, including the overlap region, consisted of the lower wall and the fluid up to z_0 in Fig. 2 ($\sim$14 molecular diameters). The continuum computation modeled the fluid from the HSI to the upper wall. To simplify the analysis, the HSI was oriented parallel to the walls. This ensured that the time-averaged mass flux was tangential to the MD-continuum interface.

In the MD region, the fluid was modeled as an isothermal ensemble of N_f spherical particles. Particles separated by distance r interacted via a shifted Lennard-Jones (LJ) potential truncated at $r=r_c$,

$$V^{\mathrm{LJ}}(r)=4\epsilon\left[\left(\frac{\sigma}{r}\right)^{12}-\left(\frac{\sigma}{r}\right)^{6}-\left(\frac{\sigma}{r_c}\right)^{12}+\left(\frac{\sigma}{r_c}\right)^{6}\right], \qquad (1)$$

where ϵ and σ are characteristic energy and length scales. The wall consisted of N_w atoms forming two (111) planes of an fcc lattice oriented with the $(11\bar{2})$ direction along $\hat{x}$. The wall-fluid interaction was also modeled with a truncated LJ potential [Eq. (1)] with parameters ϵ^{wf}, σ^{wf}, and r_c^w. Similar models have been widely used to study fluid flow in bulk and interfacial geometries [1,2]. The equations of motion were integrated using a fifth-order Gear predictor-corrector algorithm with a time step $\Delta t_{\mathrm{MD}}=0.005\tau$, where $\tau=(m\sigma^2/\epsilon)^{1/2}$ is the characteristic time of the LJ potential [6].

A constant temperature T was maintained by weakly coupling the y component of the particle velocity to a thermal reservoir. This coupling was modeled by adding Langevin noise and frictional terms to the equation of motion [7]. To terminate the spatial extent of the MD computation and fix the density ρ in the vicinity of the HSI, a constant external field $\vec{F}_{ext}=-\alpha P\rho^{-2/3}\hat{z}$ was applied to the outermost overlap particles with position $z>z_0$. P is the thermodynamic pressure of the continuum, and α is a constant of order 1 that controls the amount of structure induced in the vicinity of z_0.

In the continuum region of the computation, the dynamics of the fluid was modeled using the Navier-Stokes (NS) equation with constant viscosity μ and density ρ. Since the flow is unidirectional, the equation of motion becomes

$$\rho\frac{\partial v_x}{\partial t}=\mu\frac{\partial^2 v_x}{\partial z^2}. \qquad (2)$$

This equation was integrated using an explicit, finite-differencing approximation with grid spacing Δz_{NS} and time step $\Delta t_{\mathrm{NS}}\leq\rho\Delta z_{\mathrm{NS}}^2/2\mu$ [8]. At the static top wall, a no-slip flow BC was used. At the HSI, the flow boundary condition was supplied by the MD computation by averaging the x component of the particle velocities within a bin of width Δz centered about the HSI (the zeroth bin in Fig. 1). For the results presented below, $\Delta z\approx 1\sigma$.

As discussed above, stress continuity at the HSI was achieved by constraining the dynamics of the overlap particles. In the context of Fig. 1, the overlap particles correspond to those in bins labeled greater than 0. For particles in the jth bin (of width Δz), this constraint may be expressed as

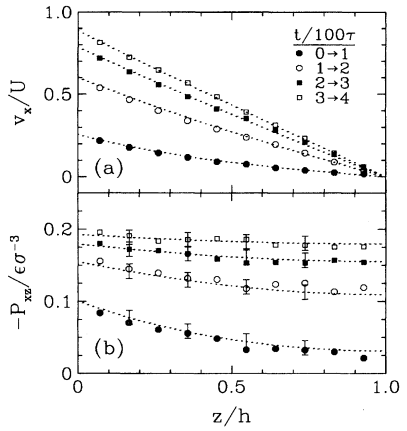

FIG. 3. Time evolution of (a) fluid velocity v_x and (b) shear stress P_{xz} in the startup flow problem [12]. Symbols denote MD results obtained by averaging instantaneous values within bins of width 2σ over 100τ intervals. Dotted lines denote the corresponding solution of Eq. (2).

$$\sum_{n=1}^{N_j} p_n - M^{(j)} v_x^{(j)} = 0, \tag{3}$$

where N_j is the total number of particles in the jth bin and p_n is the momentum of the nth particle in the $\hat{x}$ direction. $M^{(j)}$ denotes the mass of the continuum fluid element corresponding to the jth bin, and $v_x^{(j)}$ is its velocity. In this form, the constraint is nonholonomic. Through an integration with respect to time, it may be recast as a holonomic constraint and directly incorporated into Lagrange's equations [9]. The resulting equations of motion for the ith particle of mass m in the jth bin ($j \geq 1$) are

$$\dot{x}_i = \frac{p_i}{m} + \xi \left[\frac{M^{(j)}}{m N_j} v_x^{(j)} - \frac{1}{N_j} \sum_{n=1}^{N_j} \frac{p_n}{m} \right],$$

$$\dot{p}_i = -\frac{\partial}{\partial x} V^{\mathrm{LJ}}. \tag{4}$$

The strength of the constraint ξ was introduced to control the rate at which the overlap particle momenta relax to the local continuum value. As discussed below, an appropriate value for this parameter must take into account the correlation times of the particle dynamics.

To establish a base line with which to compare the hybrid results, we first carried out a full MD simulation of the flow. This entailed modeling both walls at the atomistic level and including fluid particles across the entire cell. The cell measured $h = 20.6\sigma$ between the walls and 12.5σ by 7.2σ in the xy plane. The system parameters were $N_f = 1440$, $N_w = 144$, $\epsilon^{wf} = 0.6\epsilon$, $\sigma^{wf} = \sigma$, and $r_c^w = r_c = 2.2\sigma$ [11]. A similar system has been studied extensively elsewhere under both equilibrium and nonequilibrium conditions [2]. At $T = 1.1\epsilon/k_B$ and $\rho = 0.81\sigma^{-3}$, the fluid is in a well-defined liquid phase with $\mu = 2.14\epsilon\tau\sigma^{-3}$.

To induce shear within the film, the lower wall was translated in the $\hat{x}$ direction with velocity $v_w(t)$ $= U[1 - \exp(-t/t_0)]$, where $U = 2\sigma\tau^{-1}$ and $t_0 = 160\tau$ [13]. Note that t_0 was large enough to ensure that the local shear rate in the fluid was $< 0.1\tau^{-1}$. The time evolution of the resulting velocity and stress fields is shown in Fig. 3. The dotted lines denote profiles obtained by solving Eq. (2) for a fluid with the same ρ and μ as the MD and assuming a no-slip BC at both walls. Representative error bars are shown in Fig. 3(b) to reflect the fluctuations observed about this solution for five independent runs [14]. The results demonstrate that, despite strong variations in particle density near the wall, both the velocity and stress fields for the MD simulation are in excellent agreement with the continuum solution. Due to this agreement, we used the continuum profiles as the base line with which to evaluate the performance of the hybrid code.

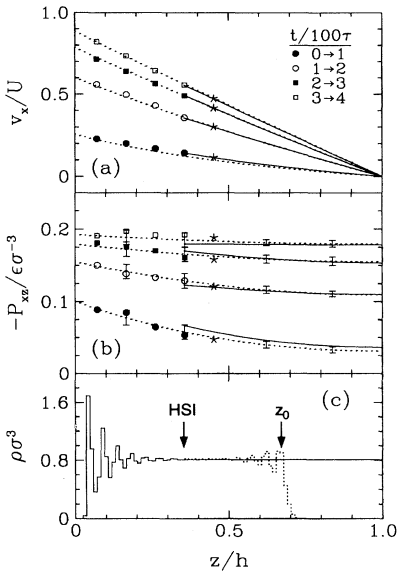

FIG. 4. Time evolution of (a) velocity and (b) stress fields in the startup flow. Symbols and solid lines denote hybrid solution averaged over 100τ intervals. Starred points indicate values at $\sim 2\sigma$ into the overlap region. Dotted lines denote the solution of Eq. (2). The bin-averaged fluid density is shown in (c), where the dotted line represents the overlap.

The solution for the startup flow obtained using the hybrid code is shown in Fig. 4 [13]. As described above, only the lower portion of the cell was modeled at the particle level. This included one wall with $N_w = 144$ and the adjacent fluid with $N_f = 1008$. A density profile averaged over the duration of the run (400τ) is shown in Fig. 4(c). The density oscillations near the lower wall typify the microscopic structure observed in fluids at solid interfaces [1,2]. In general, the magnitude of the oscillations decays with increasing z, and ρ approaches its bulk value at ~ 5–6 molecular diameters from the wall. We located the HSI within this bulk region at $z = 0.35h$. The dotted line in Fig. 4(c) for $z > 0.35h$ denotes the density distribution for the overlap particles. Note that the external field $\vec{F}_{ext}$, applied at position $z_0 = 0.67h$ with $\alpha = 2$ and $P = 3\epsilon\sigma^{-3}$, induced only small oscillations in the particle density. This significantly reduced the size of the overlap needed to provide continuity at the HSI. To obtain

good results, we find that continuity of density must extend a few r_c into the overlap region [10].

Results for the velocity and stress fields are shown in Figs. 4(a) and 4(b). Note that the magnitudes of the error bars are the same as those reported for the full MD simulations [14]. The results were obtained with $\Delta z_{\mathrm{NS}}=1.1\sigma$, $\Delta t_{\mathrm{NS}}=\Delta t_{\mathrm{MD}}$, and $\xi=0.01$. Smaller values of ξ provided an inadequate coupling between the MD and continuum. Larger values led to excessive damping of particle fluctuations and caused substantial deviations from the base line solution [10]. In general, we obtained the best results for couplings with values of $\Delta t_{\mathrm{MD}}/\xi$ slightly larger than the characteristic decay time t_{vv} of the particle velocity auto-correlation function. For a LJ liquid at $\rho=0.81\sigma^{-3}$ and $T=1.1\epsilon/k_B$, $t_{vv}\sim 0.14\tau$.

The excellent agreement within statistical fluctuations between the hybrid solution and the base line for the velocity and stress fields demonstrates the validity of our hybrid algorithm. This agreement requires the flow solution to be consistent with the continuum only in the vicinity of the HSI. The starred points in Figs. 4(a) and 4(b) demonstrate that this condition is met at $\sim 2\sigma$ into the overlap region. They indicate that continuity across the HSI can be achieved despite the local distortion of fluid structure and stress in the outermost portion of the overlap region. This fact gives tremendous flexibility in modeling the overlap which will prove useful in adapting the algorithm to flows in more complex geometries. Of particular interest are interfacial flows, such as the spreading of a fluid on a solid substrate, where poorly understood microscopic effects control the macroscopic behavior [1,15].

Although we have restricted our discussion to simple fluids, the algorithm may be readily applied to complex liquids. This stems from the fact that the constraint dynamics used to couple the discrete and continuum computations in the overlap region allow for a consistent stress regardless of the molecular potential. For example, to model polymer melts, only those monomers within the overlap region need be constrained. The only restriction is that the extent of the overlap region must reflect the range of the potential.

S.T.O. thanks the National Science Foundation for financial support, and P.A.T. thanks the Exxon Education Foundation for their generous support.

[1] J. Koplik and J. R. Banavar, Annu. Rev. Fluid Mech. **27**, 257 (1995) and references therein.

[2] P. A. Thompson and M. O. Robbins, Phys. Rev. A **41**, 6830 (1990).

[3] F. J. de Jong, J. S. Sabnis, and R. C. Buggeln, J. Spacecr. Rockets **29**, 312 (1992); T. J. Sommerer and M. J. Kushner, J. Appl. Phys. **71**, 1654 (1992).

[4] D. C. Wadsworth and D. A. Erwin, American Institute of Aeronautics and Astronautics Report No. 90-1690, 1990 (unpublished).

[5] See, for example, G. K. Batchelor, *An Introduction to Fluid Dynamics* (Cambridge University Press, Cambridge, 1967).

[6] M. Allen and D. Tildesley, *Computer Simulation of Liquids* (Clarendon Press, Oxford, 1987).

[7] G. S. Grest and K. Kremer, Phys. Rev. A **33**, 3628 (1986).

[8] W. H. Press *et al.*, *Numerical Recipes in FORTRAN*, 2nd ed. (Cambridge University Press, Cambridge, 1992).

[9] H. Goldstein, *Classical Mechanics* (Addison-Wesley, Menlo Park, 1980).

[10] S. T. O'Connell and P. A. Thompson (unpublished).

[11] These LJ parameters yield a no-slip BC at the walls [2].

[12] P_{xz} denotes the xz component of the microscopic stress tensor [6].

[13] The fluid was equilibrated for 100τ prior to shearing.

[14] In Figs. 3 and 4, v_x error bars are the size of the symbols.

[15] P. A. Thompson and M. O. Robbins, Phys. World **3**, 35 (November 1990); P. A. Thompson, W. B. Brinkerhoff, and M. O. Robbins, J. Adhesion Sci. Technol. **7**, 535 (1993).